Science Signaling
AAAS

www.sciencesignaling.org/cgi/content/full/10/473/eaai7696/DC1

Supplementary Materials for

Astrocyte-shed extracellular vesicles regulate the peripheral leukocyte response to inflammatory brain lesions

Alex M. Dickens, Luis B. Tovar-y-Romo, Seung-Wan Yoo, Amanda L. Trout, Mihyun Bae, Marlene Kanmogne, Bezawit Megra, Dionna W. Williams, Kennith W. Witwer, Mar Gacias, Nino Tabatadze, Robert N. Cole, Patrizia Casaccia, Joan W. Berman, Daniel C. Anthony, Norman J. Haughey*

*Corresponding author. Email: nhaughe1@jhmi.edu

Published 4 April 2017, *Sci. Signal.* **10**, eaai7696 (2017)
DOI: 10.1126/scisignal.aai7696

The PDF file includes:

Other Supplementary Material for this manuscript includes the following:
(available at www.sciencesignaling.org/cgi/content/full/10/473/eaai7696/DC1)

Table S2 (Microsoft Excel format). List of all proteins identified in exosomes collected from IL-1β–stimulated GFAP-GFP astrocytes.
Movie S1 (.mov format). Visualization of IL-1β–induced release of EVs from cultured primary astrocytes.

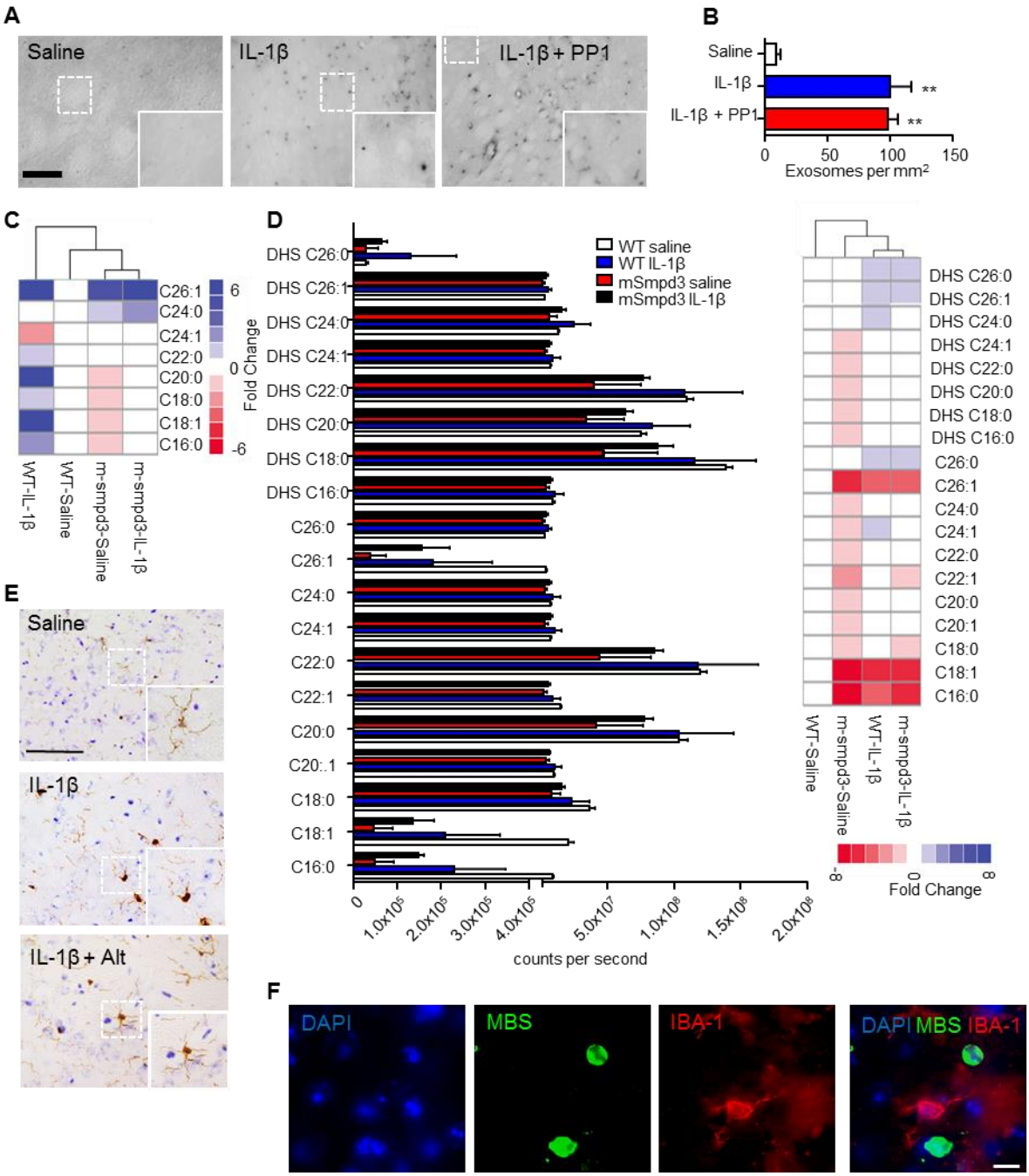

Fig. S1. Additional leukocyte, ceramide, and sphingomyelin measurements. (**A**) Representative photomicrographs of Ly6b+ leukocytes in striatum 24 hours after injection of saline, IL-1β (0.1 ng in 3 μl), or IL-1β + PP1 (0.176 ng in 3 μl). Insets are magnifications of the indicated regions. Scale bar = 250 μm. (**B**) Stereological quantitations for the indicated treatments. (**C**) Hierarchical clustering analysis of ceramide species (identified by acyl chain length and saturation) in striatum 2 hours after the indicated treatments. (**D**) Quantitative mass spectrometry and hierarchical clustering of dihydrosphingomyelin and sphingomyelin species (identified by acyl chain length and saturation) 2 hours after the indicated treatments. (**E**) Representative photomicrographs of Iba-1+ microglia in striatum in Wt mice. Insets show a ramified quiescent microglia in Saline injected, amoeboid activated microglia in IL-1β, and ramified microglia in IL-1β + Altenusin. (**F**) Immunofluorescent staining of striatum in Wt mice 24 hours following injection of IL-1β showing that MBS+ leukocytes do not overlap with Iba-1+ microglia. Nuclei are identified with DAPI. Data are mean ± SEM, n = 3-6 mice per condition. ** $p < 0.01$ compared to control.

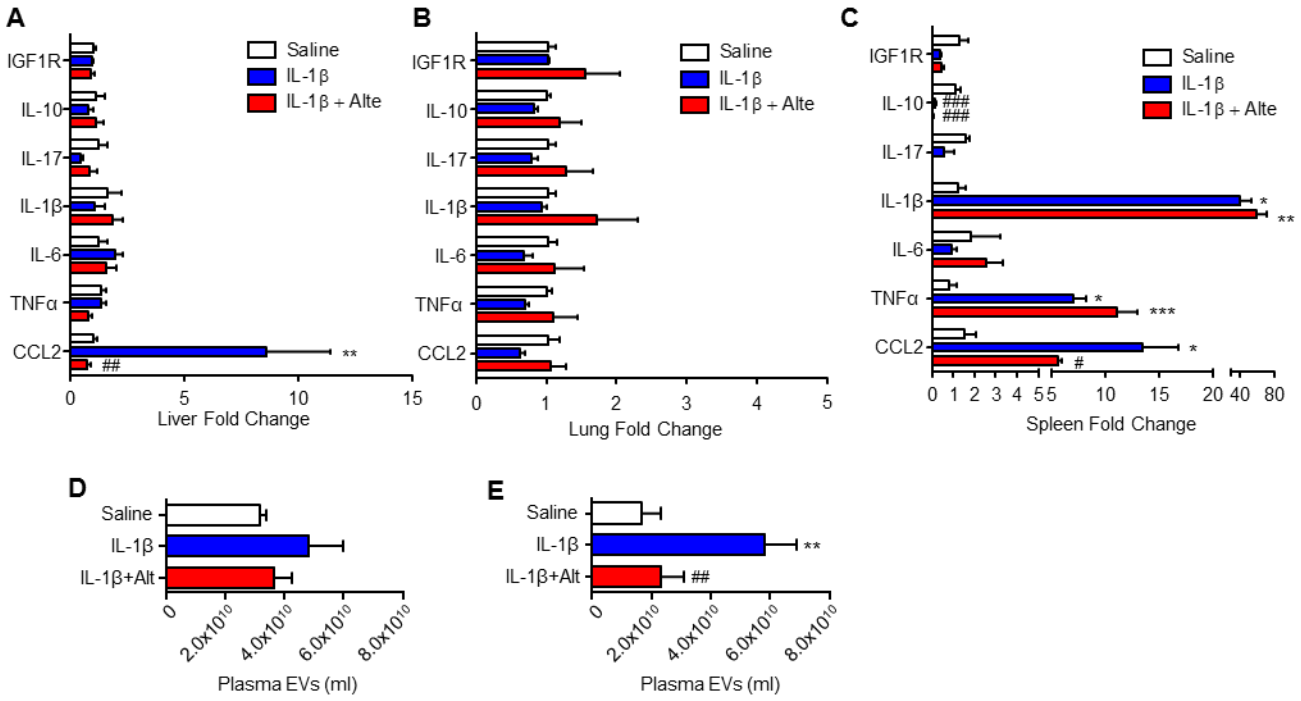

Fig. S2. Additional cytokine measurements and plasma EV counts after intrastriatal injection of IL-1β. Cytokine expression in (**A**) liver (**B**) lung, and (**C**) spleen measured 24 hours following intra-striatal injections of saline, IL-1β (0.1 ng in 3 μl), or IL-1β + altenusin (50 μM). EVs were quantified in plasma of mice (**D**) 2 hours, and (**E**) 24 hours following intra-striatal injections of saline, IL-1β, or IL-1β + altenusin. Data are mean ± SEM, n = 3-6 mice per condition. * $p < 0.05$, ** $p < 0.01$, *** $p < 0.001$ compared to control, and $^{\#}p < 0.05$, $^{\#\#}p < 0.01$, $^{\#\#\#}p < 0.001$ compared to IL-1β.

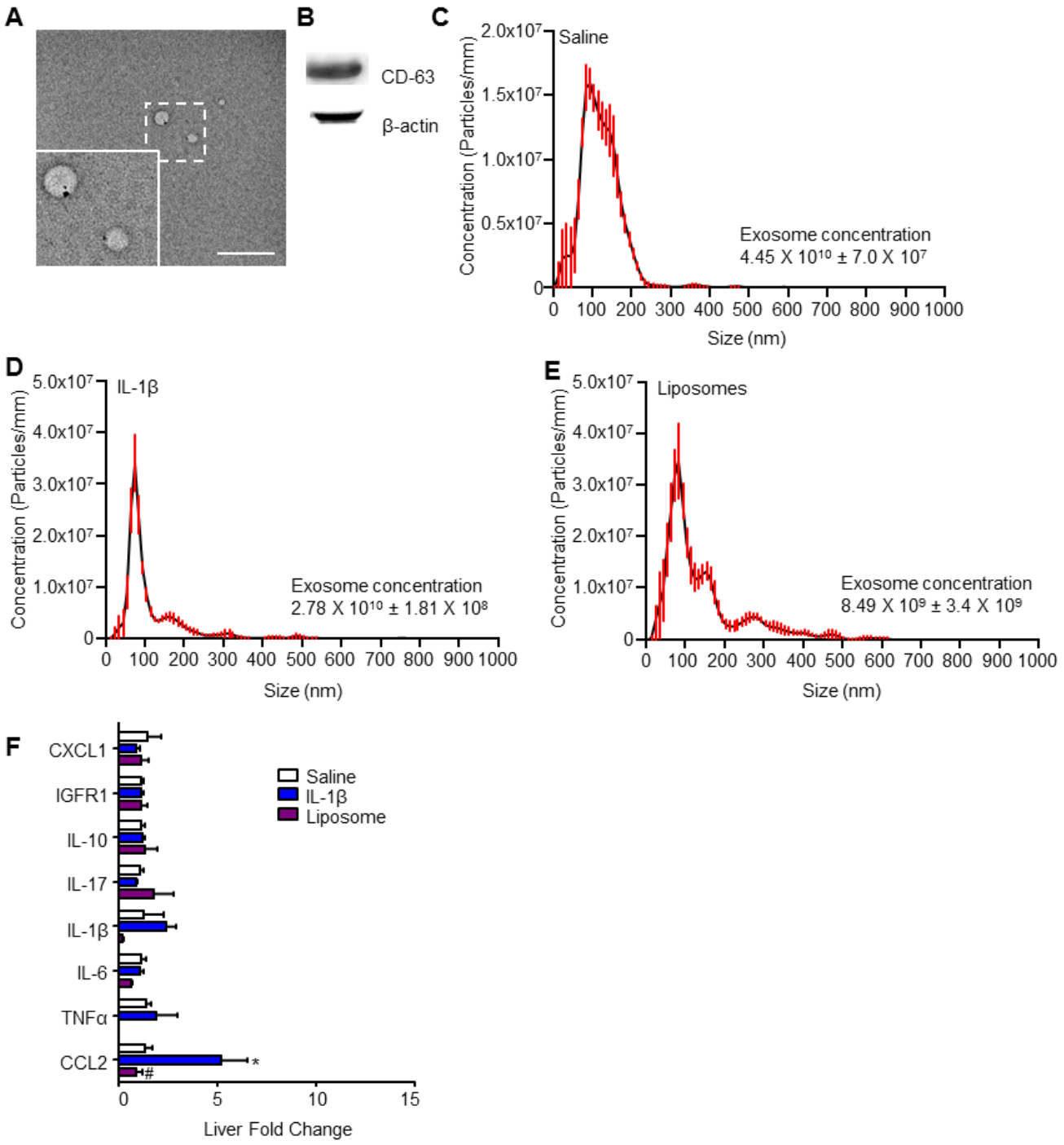

Fig. S3. EV isolation, quantitation, and liver cytokine response 24 hours after EV infusion in mice. (**A**) Representative electron micrograph of EV isolated from plasma. Scale bar = 100 μm. (**B**) Western blot showing that EV were immunopositive for the tetraspan protein marker of EV CD63. (**C**-**E**) Nanoparticle tracking showing size and concentration of EV isolated from serum 2 hours after striatial injection of (C) saline (D) IL-1β or (E) protein and RNA depleted EV (liposomes). (**F**) Liver cytokine expression 24 hours after tail vein infusion of 3.0 X 10^9 EV or liposomes into recipient animals co-injected in striatum with IL-1β (0.1 ng in 3 μl) + altenusin (50 μM). Data are mean ± SEM, n = 4-10 mice per condition. * $p < 0.05$ compared to control, and $^{\#}$ $p < 0.05$ compared to IL-1β.

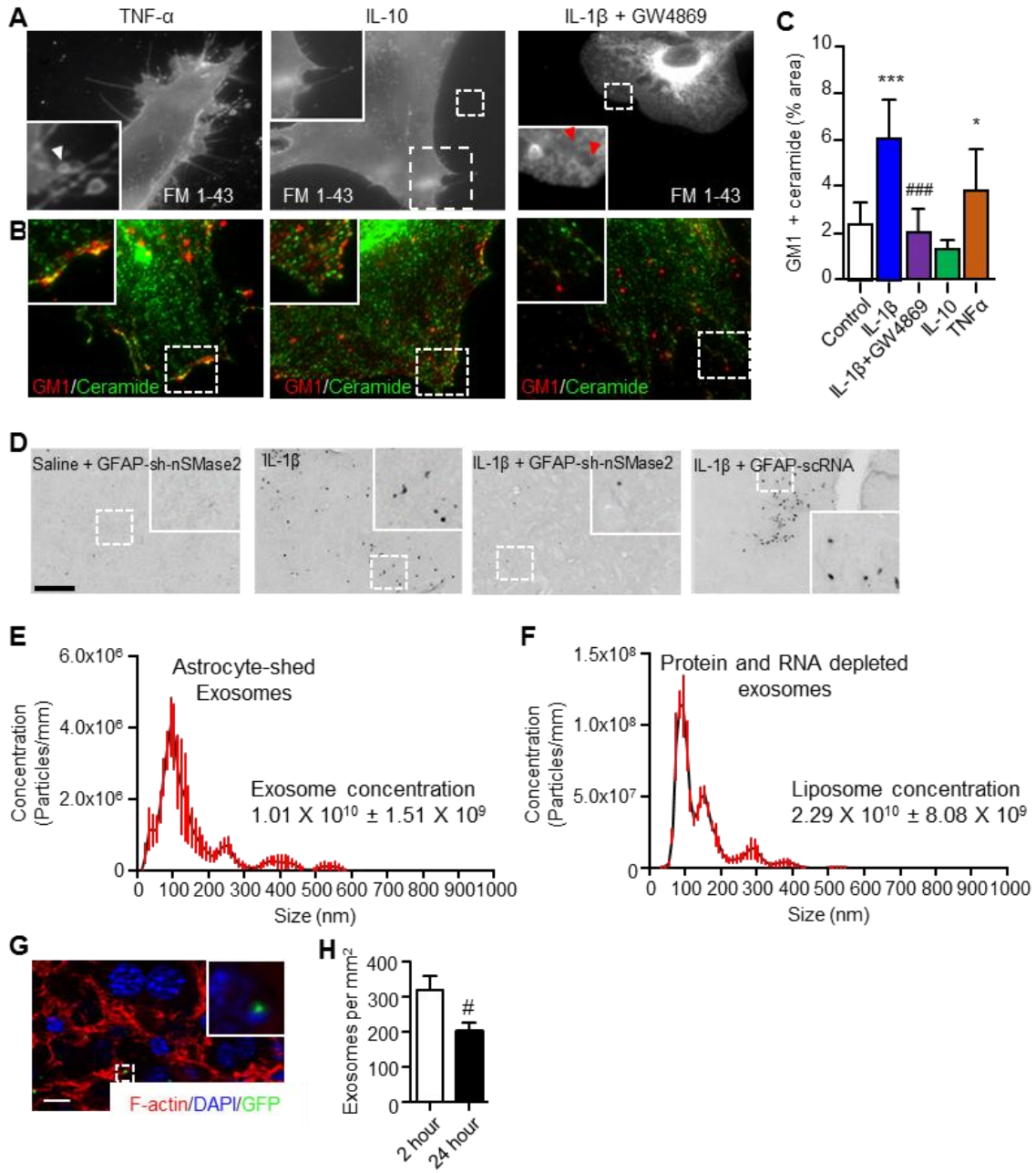

Fig. S4. IL-1β and TNFα promote formation of ceramide-rich membrane microdomains and EV release from astrocytes. (**A**) Representative fluorescence images from FM1-43 labeled astrocytes showing that TNFα (100 ng/ml), but not IL-10 (100 ng/ml) stimulated a rapid (within 2 min) release of EV (white arrows). Inhibition of nSMase with GW4869 (20 μM) blocked IL-1β stimulated release of EV, but did not prevent the formation of multivesicular bodies (red arrows). (**B**) Representative immunofluorescent images and (**C**) quantitation of plasma membrane dual positive for GM1/ceramide. IL-1β induced a rapid formation of CTX555 (labels the ganglioside GM1; red), and ceramide (green) dual positive plasma membrane microdomains. Microdomain formation was blocked by pre-treatment with GW4869. A similar result was obtained with TNFα that is also known to be associated with the nSMase2-mediated formation of ceramide, but not the anti-inflammatory cytokine IL10 that is not linked to nSMase2. (**D**) Representative photomicrographs of Ly6b+ leukocytes in striatum 24 hours after administration of saline, IL-1β, IL-1β + GFAP-sh-nSMase2 (5 x 10^9 particles in 0.5 μl), IL-1β + scRNA (scrambled sequence; 5 x 10^9 particles in 0.5 μl). (**E** and **F**) Nanoparticle tracking analysis showing size, distribution, and concentration (inset) of EV isolated from GFAP-GFP astrocytes in response to IL-1β (100 ng/ml stimulation) (E), and protein + RNA depleted EV (F). (**G**) Merged image (2 hours) and (**H**) stereological quantitation (2 hours, 24 hours) in liver following tail vein infusion of 3.0 X 10^9 GFP+ EV. F-actin labeled cells (red), DAPI labeled nuclei (blue), and GFP+ EV (green). Insets are magnifications of the indicated regions. Scale bar = 250 μm. Data are mean ± S.D, n = 10 experiments for tissue culture, and n = 3 mice per condition. * = $p < 0.05$, *** $p < 0.001$ compared to control, $^{\#}$ = $p < 0.05$, $^{\#\#\#}$ = $p < 0.001$ compared to IL-1β. ANOVA with Tukey post-hoc comparisons.

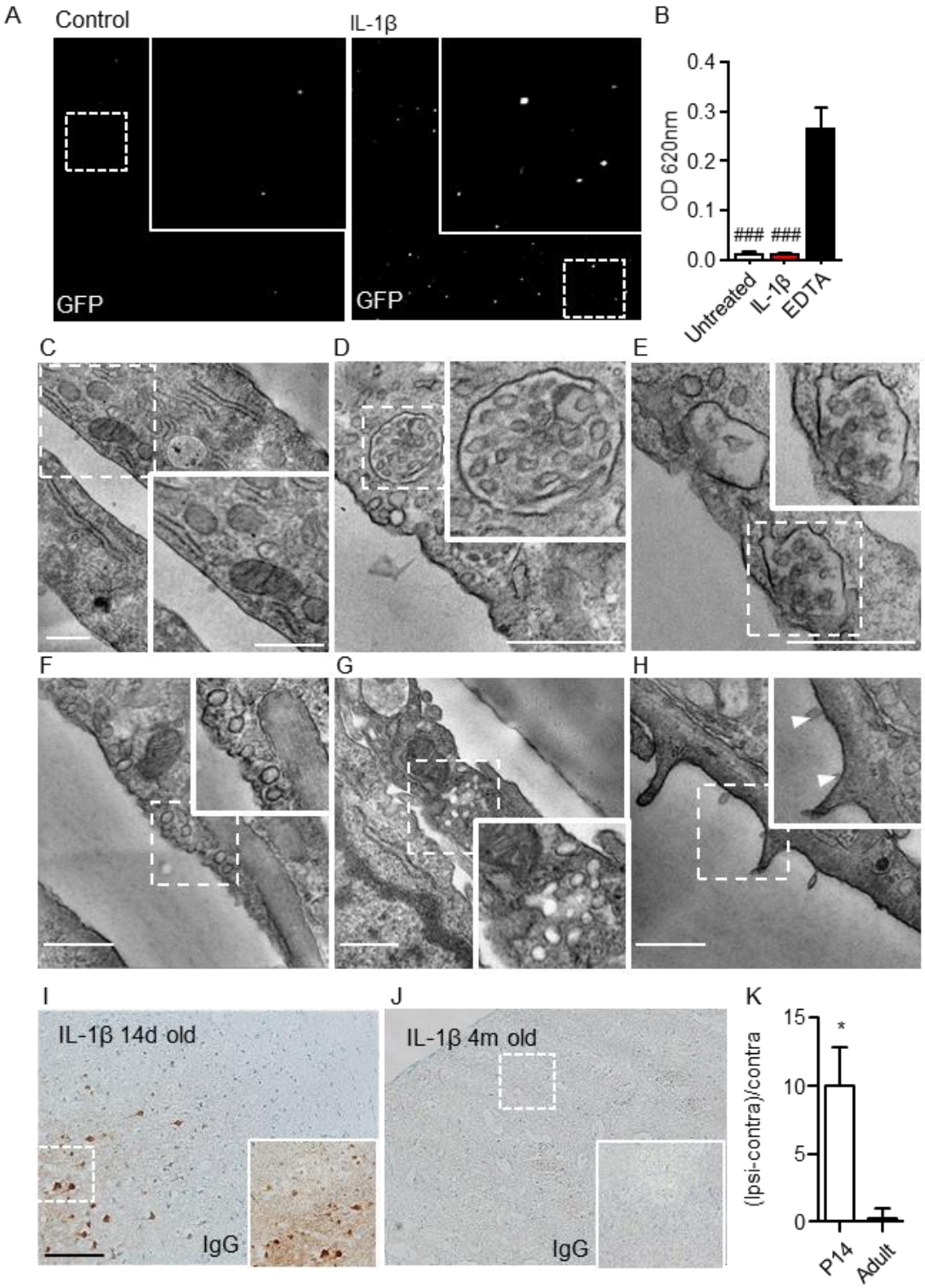

Fig. S5. EVs rapidly transverse endothelial cells in a BBB model system. (**A**) Representative images of GFP+ EV collected from the luminal side of the BBB culture following stimulation of the astrocyte side of the bilayer with vehicle (Control) or IL-1β (100 ng/ml). Insets show magnifications of the indicated regions. IL-1beta treatment did not cause BBB permeability as assayed by (**B**) passage of Evan's blue dye coupled BSA. Representative electron micrographs from BBB cultures showing (**C**) an astrocyte under control conditions, (**D**) multivesicular bodies are apparent astrocytes within 15 min following stimulation with IL-1β (100 ng/ml), that (**E**) fuse with the plasma membrane, (**F**) are taken up by endothelium, (**G**) transverse the cytoplasm, and (**H**) are released site on the luminal side of the endothelium (white arrows show EV in the process of being released) Inserts show magnification of the indicated region. Representative images show IgG immunostaining in striatum from (**I**) 14 day old, and (**J**) 4 month old mice injected in striatum with IL-1β (0.1 ng in 3 μl) and (**K**) quantitative results. Scale bar = 100 nm. Data are mean ± SEM, n = 3 mice or measurement per condition. * = $p < 0.05$ compared to adult mice, $^{###}$ = $p < 0.001$ compared to EDTA. ANOVA with Tukey post-hoc comparisons.

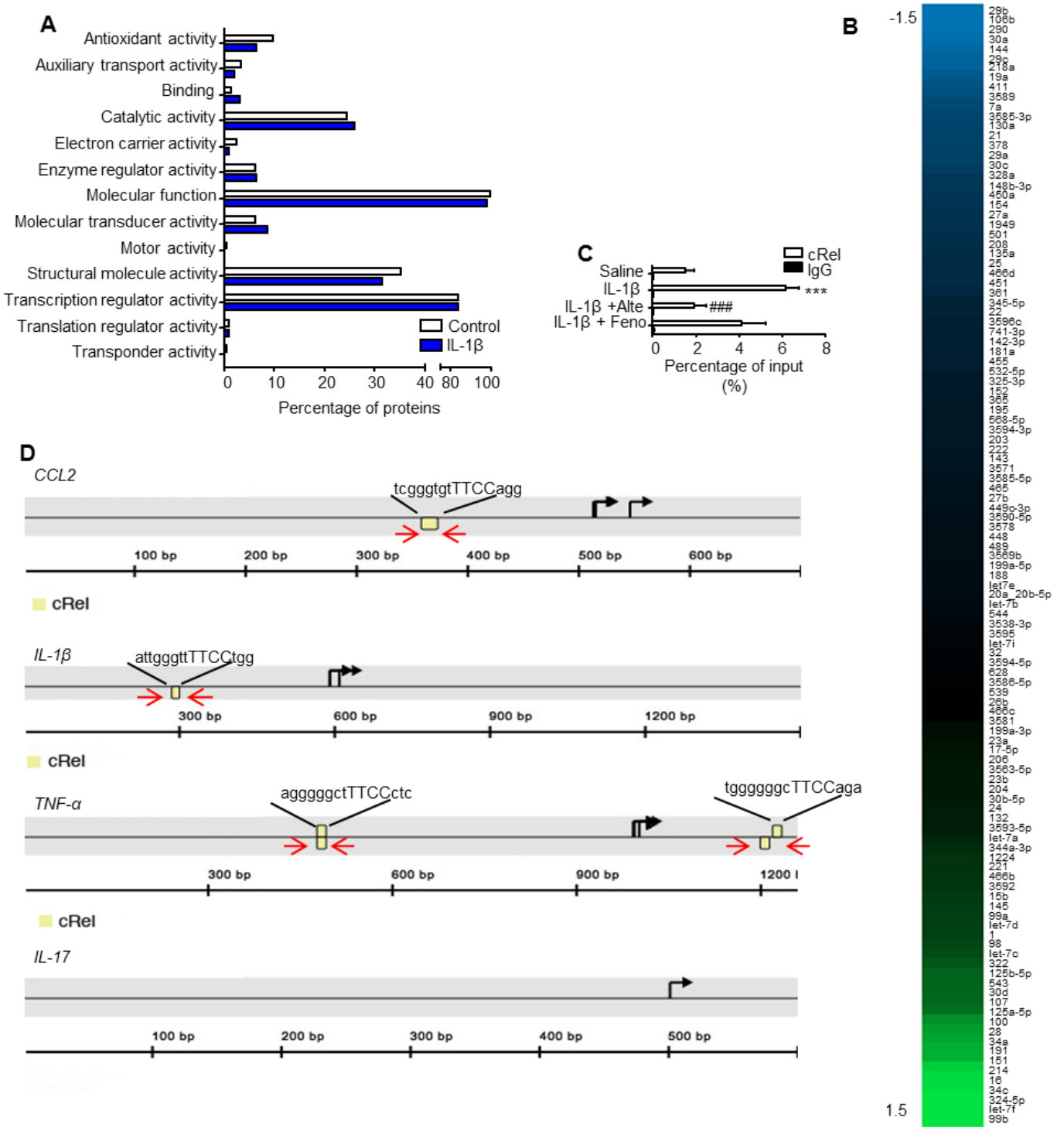

Fig. S6. Additional proteomic and ChIP results. (**A**) Proteins detected in EV were largely related to molecular function, catalytic activity and binding. (**B**) Heat map of quantile normalized data from NanoString hybridization assay. We detected 124 miRNAs two standard deviations or more above background measures defined by six negative controls. Green color indicates upregulated miRNAs, and blue indicates downregulated miRNAs compared with control (log2 scale). (**C**) ChIP assays results showing increased NF-κB binding to a second promotor region of TNF-α in liver following striatal injection of IL-1β (1 ng in 3 µl) compared to the saline. Co-administration of IL-1β + altenusin (50 µM) prevented NF-κB binding to this promoter region. (**D**) Pictorial representations of the binding regions used in the ChIP assay. Data are mean ± SEM, n = 3 mice per condition. *** $p < 0.001$ compared to control, $^{###}$ = $p < 0.001$ compared to IL-1β. ANOVA with Tukey post-hoc comparisons.

Table S1. List of all proteins identified in exosomes collected from control GFAP-GFP astrocytes. The table is provided as an Excel file in the auxiliary materials online.

Table S2. List of all proteins identified in exosomes collected from IL-1β–stimulated GFAP-GFP astrocytes. The table is provided as an Excel file in the auxiliary materials online.

Table S3. List of miRNA identified in exosomes and relative fold change. The miRNA content of extracellular vesicles released cultured astrocytes upon stimulation with IL-1β or released over a 24 hour period was measured using a NanoString multiplex system. The fold change was then calculated by dividing the normalised miRNA counts from the IL-1β EVs by the normalised counts from the control EVs.

miRNA identity	Accession number	IL-1β/ctl ratio
rno-let-7a	MIMAT0000774	0.241345887
rno-let-7b	MIMAT0000775	-0.104969975
rno-let-7c	MIMAT0000776	0.485001547
rno-let-7d	MIMAT0000562	0.351745631
rno-let-7e	MIMAT0000777	-0.11668322
rno-let-7f	MIMAT0000778	3.186973671
rno-let-7i	MIMAT0000779	-0.032254872
rno-miR-1	MIMAT0003125	0.393657805
rno-miR-100	MIMAT0000822	1.051643749
rno-miR-106b	MIMAT0000825	-0.661234696
rno-miR-107	MIMAT0000826	0.668524345
rno-miR-1224	MIMAT0012827	0.270175787
rno-miR-125a-5p	MIMAT0000829	0.938402599
rno-miR-125b-5p	MIMAT0000830	0.584757329
rno-miR-126	MIMAT0000832	-0.062153451
rno-miR-130a	MIMAT0000836	-0.471077818
rno-miR-132	MIMAT0000838	0.151302286
rno-miR-135a	MIMAT0000841	-0.342751409
rno-miR-142-3p	MIMAT0000848	-0.252981614
rno-miR-143	MIMAT0000849	-0.196021933
rno-miR-144	MIMAT0000850	-0.622644233
rno-miR-145	MIMAT0000851	0.346288928
rno-miR-148b-3p	MIMAT0000579	-0.398725668
rno-miR-151	MIMAT0000613	1.596999376
rno-miR-152	MIMAT0000854	-0.214297227
rno-miR-154	MIMAT0000856	-0.385053867
rno-miR-15b	MIMAT0000784	0.321288628
rno-miR-16	MIMAT0000785	1.764426981
rno-miR-17-5p	MIMAT0000786	0.121077642
rno-miR-181a	MIMAT0000858	-0.247270899
rno-miR-188	MIMAT0005301	-0.11951032
rno-miR-190b	MIMAT0005302	-0.967210493
rno-miR-191	MIMAT0000866	1.259744602
rno-miR-1949	MIMAT0017852	-0.368446812
rno-miR-195	MIMAT0000870	-0.206075705
rno-miR-199a-3p	MIMAT0004738	0.095284716
rno-miR-199a-5p	MIMAT0000872	-0.123404364
rno-miR-19a	MIMAT0000789	-0.567524871

miRNA identity	Accession number	IL-1β/ctl ratio
rno-miR-203	MIMAT0000876	-0.201029178
rno-miR-204	MIMAT0000877	0.130302957
rno-miR-206	MIMAT0000879	0.121388133
rno-miR-208.017	MIMAT0000880	-0.351104424
rno-miR-20a+rno-miR-20b-5p	MIMAT0000602	-0.109971728
rno-miR-21	MIMAT0000790	-0.464284125
rno-miR-214	MIMAT0000885	1.762106811
rno-miR-218a	MIMAT0000888	-0.598528223
rno-miR-22	MIMAT0000791	-0.274139644
rno-miR-221	MIMAT0000890	0.280706397
rno-miR-222	MIMAT0000891	-0.201029178
rno-miR-23a	MIMAT0000792	0.102005439
rno-miR-23b	MIMAT0000793	0.128391443
rno-miR-24	MIMAT0000794	0.14643189
rno-miR-25	MIMAT0000795	-0.331260552
rno-miR-26b	MIMAT0000797	0.006233158
rno-miR-27a	MIMAT0000799	-0.379693253
rno-miR-27b	MIMAT0000798	-0.159528393
rno-miR-28	MIMAT0000800	1.131952445
rno-miR-290.028	MIMAT0000893	-0.654170672
rno-miR-293	MIMAT0012847	-0.968854452
rno-miR-29a	MIMAT0000802	-0.450265874
rno-miR-29b	MIMAT0000801	-0.681164638
rno-miR-29c	MIMAT0000803	-0.599276754
rno-miR-301a	MIMAT0000552	-0.080720933
rno-miR-30a	MIMAT0000808	-0.637919462
rno-miR-30b-5p	MIMAT0000806	0.144706947
rno-miR-30c	MIMAT0000804	-0.449857491
rno-miR-30d	MIMAT0000807	0.616652495
rno-miR-32	MIMAT0000811	-0.0212707
rno-miR-322	MIMAT0001619	0.576101993
rno-miR-324-5p	MIMAT0000553	2.478249832
rno-miR-325-3p	MIMAT0004639	-0.239408304
rno-miR-328a	MIMAT0000564	-0.434663384
rno-miR-335	MIMAT0000575	-0.962989709
rno-miR-344a-3p	MIMAT0000592	0.269079204
rno-miR-345-5p	MIMAT0000594	-0.301188957
rno-miR-34a	MIMAT0000815	1.234647452
rno-miR-34c	MIMAT0000814	2.474663256
rno-miR-3563-5p	MIMAT0017833	0.121788183
rno-miR-3571	MIMAT0017851	-0.18686897
rno-miR-3578	MIMAT0017866	-0.138915464
rno-miR-3581	MIMAT0017870	0.07029518
rno-miR-3583-3p	MIMAT0017874	-0.082914689
rno-miR-3585-3p	MIMAT0017879	-0.479606403
rno-miR-3585-5p	MIMAT0017878	-0.183745092
rno-miR-3586-5p	MIMAT0017880	-0.008821139
rno-miR-3589	MIMAT0003379	-0.515453797
rno-miR-3590-3p	MIMAT0017890	-0.048680908
rno-miR-3590-5p	MIMAT0017889	-0.151199488

miRNA identity	Accession number	IL-1β/ctl ratio
rno-miR-3592	MIMAT0017895	0.314053506
rno-miR-3593-5p	MIMAT0017896	0.194009308
rno-miR-3594-3p	MIMAT0017899	-0.201666761
rno-miR-3594-5p	MIMAT0017898	-0.021090167
rno-miR-3595	MIMAT0017903	-0.042135419
rno-miR-3596b	MIMAT0017871	-0.124293553
rno-miR-3596c	MIMAT0017877	-0.272721368
rno-miR-361	MIMAT0003117	-0.325117714
rno-miR-365	MIMAT0001549	-0.211966209
rno-miR-378	MIMAT0017888	-0.457356575
rno-miR-411	MIMAT0005312	-0.540763615
rno-miR-421	MIMAT0001320	-0.057591482
rno-miR-448	MIMAT0001534	-0.132958072
rno-miR-449c-3p	MIMAT0017804	-0.153123849
rno-miR-450a	MIMAT0001547	-0.394606342
rno-miR-451	MIMAT0001633	-0.325318319
rno-miR-455	MIMAT0005316	-0.245761095
rno-miR-465	MIMAT0012850	-0.165802324
rno-miR-466b	MIMAT0005278	0.286337471
rno-miR-466c.039	MIMAT0005279	0.065758376
rno-miR-466d	MIMAT0017824	-0.328821749
rno-miR-489	MIMAT0003113	-0.125760338
rno-miR-501	MIMAT0003116	-0.361549945
rno-miR-511	MIMAT0012829	-0.973206117
rno-miR-532-5p	MIMAT0005322	-0.243744568
rno-miR-539	MIMAT0003176	0.000696856
rno-miR-540	MIMAT0003174	-0.966940816
rno-miR-543	MIMAT0004787	0.609186114
rno-miR-544	MIMAT0012831	-0.100741533
rno-miR-598-5p	MIMAT0005324	-0.206050432
rno-miR-628	MIMAT0012836	-0.011845546
rno-miR-741-3p	MIMAT0017902	-0.254790984
rno-miR-7a	MIMAT0000606	-0.493066671
rno-miR-98	MIMAT0000819	0.420910671
rno-miR-99a	MIMAT0000820	0.350049953
rno-miR-99b	MIMAT0000821	5.504037671

Table S4. List of ChIP primers. The sequences of each primer used for ChIP analysis in this study is listed. F, forward; R, reverse.

Primer	Sequence
mCcl2_F	5- TTC CAC TTC CTG GAA ACA CC -3
mCcl2_R	5- TCA CCC TGG ATA AGT GAT GG -3
mIl1_F	5- ACT TCT GGG TGT GCA TCT ACG -3
mIl1_R	5- GGA CAA TTG TGC AGA TGG TG -3
mIl10_F	5- GGG TTT CCT TTG GGT AAC TG -3
mIl10_R	5- TGT TTC CTC CAC TCA ACC TG -3
mIl17_F	5- CTC TTC ATC CAC CTC ACA CG -3
mIl17_R	5- TCT CCC TGG ACT CAT GTT TG -3
mTNFa_F	5- AAC TCA AAC AGG GGG CTT TC -3
mTNFa_R	5- CAT CCA TGG GGG AGA ACT TAG -3
mTNFa_F4	5- ACA CCA TGA GCA CAG AAA GC -3
mTNFa_R4	5- CGC CTG GAG TTC TGG AAG -3

Movie S1. Visualization of IL-1β–induced release of EVs from cultured primary astrocytes. The shedding of EVs from primary astrocyte cultures was visualized with styryl pyridinium dye FM1-43. The movie is provided in the auxiliary materials online.